Ice Multiplication by Fragmentation of Spherical Freezing of Drops: A Theoretical Investigation

Vaughan T J Phillips, Jun-Ichi Yano

Ice Multiplication by Fragmentation of Spherical Freezing of Drops: A Theoretical Investigation

Vaughan T. J. Phillips

Department of Physical Geography, University of Lund, Lund, Sweden

Jun-Ichi Yano*

CNRM, Météo-France and CNRS, UMR 3589, 31057 Toulouse Cedex, France

Corresponding author address: CNRM, Météo-France, 42 av Coriolis, 31057 Toulouse Cedex, France.

E-mail: jiy.gfder@gmail.com

ABSTRACT

The ice multiplication by fragmentation associated with collision–freezing of supercooled drops is investigated. A zero–dimensional dynamical system describing the time evolution of the number density of the supercooled drops and the ice crystals in a mixed–phase cloud is developed. The analytical solutions of this system are derived for various asymptotic limits. Especially, when the ice fragmentation by freezing supercooled drops is considered in its isolation, a complete analytical solution is available, which shows that the originally–existed supercooled drops are simply all converted into the ice crystals multiplied by a fragmentation number per freezing. When constant generation of both supercooled drops and ice crystals is considered, the ice–crystal number tends to linearly increase with time with the rate given by the sum of the primary–ice and the the supercooled–drop sources with the latter multiplied by the fragmentation number per freezing. The study concludes that the ice multiplication by fragmentation of freezing drops can be a crucial process in certain situations. Yet its multiplication tendency is limited by availability of supercooled rain or drizzle and by whether the freezing temperature allows more than one fragment to be emitted per frozen drop so as to allow a positive feedback with collisional raindrop-freezing. When there is no more rain or drizzle, the multiplication stops. When there is copious supercooled rain initially and temperatures are optimal, then this fragmentation can be more prolific than the other multiplication processes such as the Hallett–Mossop process and the ice–ice collision process.

1. Introduction

Coincident measurements of concentrations ice particles in clouds and of active ice nucleus (IN) aerosols in the environment have shown a discrepancy by orders of magnitude, in clouds too warm for homogeneous freezing (Hobbs 1969, Auer *et al.* 1969). This has been explained in terms of fragmentation of ice. Several pathways of fragmentation have been observed in the laboratory, but their relative importance has been unclear.

One possible type of fragmentation is shattering during collision–freezing of supercooled drops. Generally the rate of freezing of a drop is limited by the rate of dissipation of latent heat. Initially, the latent heat from freezing is converted to thermal energy of the drop, raising its temperature close to 0°C almost instantaneously. In this first stage, needles of ice permeate the drop. In the subsequent stage, the latent heat flows down the gradient of temperature to the surroundings, once a steady state has been reached. The rate of dissipation to the air governs the freezing rate. The fastest rate of freezing occurs for freezing as near as possible to the drop surface. Hence, the freezing occurs from the outside inwards, with a shell of ice encasing the liquid core.

It is experimentally observed that as the ice shell thickens, the expansion on freezing can sometimes cause the shell to shatter (Wildeman *et al.* 2017). Splinters of ice can then be emitted into the air. Many ealier laboratory experiments (Latham and Mason 1961, Brownscombe and Thorndike 1968, Dye and Hobbs 1968, Hobbs and Alkezweeny 1968, Takahashi and Yalashita 1969) measured this fragmentation for drops in free-fall: See Mossop (1970) as a review. Only a few splinters are typically emitted per frozen drops (usually less than about 1-10 depending on temperature and size). On the other hand, there is a positive feedback that can lead to all supercooled drops being frozen quite quickly: as ice splinters are emitted they can grow and after a minute or so are large enough to collide efficiently with supercooled drops, freezing them.

Phillips *et al.* (2001) quantified the effect of this multiplication mechanism by raindrop-splintering for a New Mexican convective cloud. It was found that it was less prolific than the Hallett–Mossop (1974) process of rime-splintering between -3 and -8°C when cloud-droplets freeze on impact with graupel. However, Lawson *et al.* (2015) simulated another observed case with a spectral bin microphysics parcel model and found the positive feedback to account for the observed ice.

Phillips *et al.* (2018) provided a comprehensive formulation to treat rain– or drizzle–drop freezing fragmentation by pooling published data from past laboratory studies in the literature. Two modes were represented:

• Mode 1: spherical drop-freezing when incident ice particle is less massive than the drop or due to immersed IN activating, with an outer ice shell growing inwards and breaking;

• Mode 2: non-spherical drop-freezing when incident ice particle is more massive than the drop and ice particles may be present in the splash.

Only mode 1 has been observed in the lab comprehensively. For mode 2 a theoretical approach for the physics of the collision was invoked. After creating an empirical formulation for mode 1 alone, Phillips *et al.* (2018) applied it to a simulation of a composite case of deep convection from the tropical Atlantic in ICE-T (Ice in Clouds Experiment–Tropical). They found observed ice concentrations were predicted in a bin microphysical parcel model with the new schemes for an assumed probability of 50% (-10°C) for the chance of any drop in the splash containing ice due to partial freezing on impact.

The empirical scheme for numbers of secondary fragments per drop, N, from spherical drop-freezing of mode 1 was expressed by Phillips *et al.* (2018) with a 2D phase-space of drop diameter and freezing temperature. A peak of N near -15°C was observed. Construction of a zero–dimensional (0D) model of monodisperse populations of crystals, graupel (from drop-freezing)

and supercooled drops without fallout showed that the positive feedback with exponential growth of ice concentrations only occurs for $N > 1$, which is found at diameters of 0.1 mm between about -13 and -17°C, 0.2 mm (or 0.4 mm) between about -10°C and -20°C and 1.6 mm when colder than -7°C. When mode 2 was included in the 0D model, the realm of instability was extended to a wider range of temperature.

The purpose of the present paper is to extend this investigation of the efficiency of the ice fragmentation by spherical drop-freezing from such a theoretical point of view. A similar 0D dynamical system is applied for this purpose, generalized to include a source of raindrops from coalescence, as presented in the next section. By taking the similar methodologies, Yano and Phillips (2011) and Yano *et al.* (2016) have investigated the efficiency of the Hallett–Mossop and the ice–ice collision ice–multiplication processes. Yano *et al.* (2016) further list the various methodologies applicable for interpreting the behavior of a dynamical system, and in that manner, the basic nature of a given microphysical process described by the given dynamical system can be elucidated.

The most basic strategy is to develop an asymptotic expansion by assuming a certain physical parameter to be small. We emphasize that a given physical parameter may not be necessarily small arithmetically, but it can still be introduced as a small parameter in order to obtain insights to the basic behavior of the system. This most basic strategy is systematically applied in the present study. After introducing a formulation of the problem in the next section, theoretical analysis considers first the ice fragmentation process of mode 1 in its isolation in Sec. 3 and the feedbacks are quantified. General analyses are presented in Sec. 4. Obtained results are further discussed in Sec. 5.

2. 0D Model

a. Basic Assumptions

We consider a cloud at subzero temperatures consisting of supercooled drops, ice crystals, and graupel. Their number densities are designated by n_r, n_i, and n_g, respectively. Collisions between ice crystals and supercooled drops cause freezing to the latter leading to formation of graupel, associated with N (up to 10–100) secondary fragments of ice emitted by each frozen drop. The rate that supercooled drops freezes by collision of ice particles may be given by Kn_rn_i, where K is a coefficient describing the product of the collision efficiency and rate of geometric sweep-out of air volume per second (collection kernel, $\mathrm{m}^3\ \mathrm{sec}^{-1}$).

We further assume constant generations, c_0 and c_i, of supercooled rain and ice crystals, respectively. We also assume that the supercooled rain is lost by fall with a characteristic time scale of τ_f. Some of those additional processes may be turned off in the following as required.

Here, being consistent with our earlier studies (Yano and Phillips, 2011, Yano *et al.* 2016, Phillips *et al.* 2018), no spatial dimension is considered.

b. Mathematical Formulation

From the physical assumptions just introduced above, the mathematical description of this microphysical system is presented by

$$\dot{n}_r = c_0 - Kn_rn_i - n_r/\tau_f \tag{2.1a}$$

$$\dot{n}_i = c_i + KN'n_rn_i \tag{2.1b}$$

Note that the drop–freezing is initiated by capture (loss) of an ice particle, and leads to a gain of N ice particles by fragmentation so that $N' = N - 1$ more ice particles are found after drop–freezing in total per drop frozen. This means that for some conditions of drop size and freezing temperature (as reviewed by Pruppacher and Klett 1997), there can be $N' < 0$, such as at diameters less than about 0.1 mm near the optimum of -15°C and 0.5–1 mm at temperatures several degrees warmer or colder than this. For a monodisperse population of drops, when $N' < 0$, then there is capture

of splinters causing a decrease with time of the crystal concentration with incomplete freezing of the population of drops. This corresponds to a situation in reality with a continuum of drop sizes in any cloudy volume but with insufficiently numerous large drops to cause any explosion of ice concentration (Sec. 1).

Additionally, the time evolution of the graupel number, n_g, is presented by

$$\dot{n}_g = K n_r n_i - n_g/\tau_g$$

also assuming that the graupel is lost from the cloud-microphysical system by fall-out with a characteristic time–scale, τ_g. However, the graupel number, n_g, does not affect the subsequent evolution of the remaining part of the system. Thus, in the following, the evolution of n_g will not be considered.

c. Nondimensionalization

Nondimensionalization is crucial to ensure a systematic investigation of a given system, because it reduces the parameters characterizing the system to a smaller number of nondimensional parameters, thus a parameter space for the investigation is much reduced.

In the following, we add the subscript $*$ to the nondimensional variables in order to distinguish them from the dimensional variables. Here, we introduce an unspecified time scale, τ, for nondimensionalizing the time. Although the fall time–scale, τ_f, of rain is a natural choice for the scale, we retain a certain freedom for the model analysis in this manner. Thus,

$$\frac{d}{dt} = \frac{1}{\tau}\frac{d}{dt_*}. \tag{2.2}$$

The particle number densities may be nondimensionalized by

$$n_i = n_{i*}/K\tau, \tag{2.3a}$$

$$n_r = n_{r*}/KN'\tau. \tag{2.3b}$$

By substituting the expressions (2.2), (2.3a, b) into Eqs. (2.1a, b), we obtain a nondimensionalized system:

$$\dot{n}_{r*} = \hat{c}_0 - \hat{K} n_{i*} n_{r*} - \varepsilon_s n_{r*}, \tag{2.4a}$$

$$\dot{n}_{i*} = \hat{c}_i + \hat{K} n_{r*} n_{i*}. \tag{2.4b}$$

Here, we have introduced the following nondimensional parameters:

$$\hat{c}_0 = K N' \tau^2 c_0, \tag{2.5a}$$

$$\hat{c}_i = K \tau^2 c_i, \tag{2.5b}$$

$$\varepsilon_s = \tau / \tau_f. \tag{2.5c}$$

Note that $\hat{c}_0$ and $\hat{c}_i$ are the nondimensional generation rates of liquid and ice; ε_s measures the magnitude of the rain sedimentation rate. Furthermore, the dimensionless tag, $\hat{K}$, is introduced, multiplying the freezing–fragmentation terms so as to indicate a contribution of this process to the solutions. Formally $\hat{K} = 1$ by nondimensionalization when this process is present and may be set zero otherwise. Note that the time scale, τ, is defined by Eq. (3.5) below in retrospect.

3. Basic Analysis: Freezing–Drop Fragmentation Process in Isolation

As the simplest case, the shattering of ice particles by freezing drops is considered in isolation away from the other processes. We obtain this situation by setting, $\hat{c}_0 = \hat{c}_i = \varepsilon_s = 0$ in the above general system (2.4):

$$\dot{n}_{r*} = -\hat{K} n_{r*} n_{i*}, \tag{3.1a}$$

$$\dot{n}_{i*} = \hat{K} n_{r*} n_{i*}. \tag{3.1a}$$

Here, the tag, $\hat{K}$, for the ice fragmentation process is still retained. Note that there is no nondimensional parameter controlling this system. Thus, even in numerical terms, the interest of the

investigation of this system only depends on the initial condition. As seen below, the initial condition can further be normalized, because the characteristic time–scale, τ, of the system remains arbitrary due to the absence of rain sedimentation.

a. Full Solution

We identify two equilibrium solutions in this system: either $n_{r*} = 0$ or $n_{i*} = 0$ and the other number density remains an arbitrary finite value. As suggested by Yano and Phillips (2011), as well as Yano *et al.* (2016: See especially their Sec. 6.2), the standard procedure would be to perform the linear perturbation analysis against these equilibrium states for inferring the tendency of the system away from these equilibrium states.

However, in the present case, a full analytical solution is available for Eqs. (3.1a, b). This is realized by noting that the sum of the two particle number densities is conserved, as seen by taking the sum of Eqs. (3.1a, b):

$$\frac{d}{dt_*}(n_{r*} + n_{i*}) = 0. \tag{3.2}$$

In dimensional terms, the above conservation law is

$$\frac{d}{dt}(N' n_r + n_i) = 0.$$

Thus, more precisely, the sum of the number densities, weighted by the ice–fragmentation number, N', on the rain water number density, n_r, is conserved with time.

From Eq. (3.2), n_{i*} can be written in terms of n_{r*} by

$$n_{i*} = n_0 - n_{r*}, \tag{3.3}$$

where $n_0 = n_{r*}(0) + n_{i*}(0)$ is the initial total particle number. By substituting the above expression into Eq. (3.1a), we obtain a differential equation solely in terms of n_{r*}. It can be readily solved to obtain:

$$n_{r*} = (n_{r*}(0) + n_{i*}(0))(1 + \frac{n_{i*}(0)}{n_{r*}(0)} e^{\hat{K} n_0 t_*})^{-1}. \tag{3.4a}$$

Further substitution of the above solution into Eq. (3.3) leads to a solution for n_{i*}:

$$n_{i*} = (n_{r*}(0) + n_{i*}(0))(1 + \frac{n_{r*}(0)}{n_{i*}(0)} e^{-\hat{K} n_0 t_*})^{-1}. \tag{3.4b}$$

Note that the time–scale, τ, introduced above for non-dimensionalising the system remains arbitrary. Thus without loss of generality, we may set the initial condition to $n_0 = 1$, which implies that

$$\tau = K^{-1}(N' n_r(0) + n_i(0))^{-1} \tag{3.5}$$

by referring to Eq. (2.3a, b). Note that the dimensionless characteristic time-scale for the exponentials of both n_{r*} and n_{i*} is just $1/n_0$ in Eq (3.4a, b). This characteristic time-scale becomes τ when dimensionalised. In other words, the initial particle number dictates the characteristic time–scale of the system, as shown by Phillips et al. (2018). Furthermore, the behaviour of the system can be investigated systematically by solely changing the initial condition for n_{r*} as a result. The examples of time evolution for those normalizations are shown in Fig. 1.

It may also be worthwhile to note that the solutions (3.4a, b) are given in dimensional terms by:

$$n_r = (n_r(0) + n_i(0)/N')[1 + \frac{n_i(0)}{N' n_r(0)} e^{K(N' n_r(0) + n_i(0))t}]^{-1} \tag{3.6a}$$

$$n_i = (N' n_r(0) + n_i(0))[1 + \frac{N' n_r(0)}{n_i(0)} e^{-K(N' n_r(0) + n_i(0))t}]^{-1} \tag{3.6b}$$

The result shows that regardless of the initial condition, the system exponentially approaches to a state only with the ice crystals, $n_i = N' n_r(0) + n_i(0)$ by converting all the supercooled drops into the ice. As a result, we also see that the state with $n_r \neq 0$ and $n_i = 0$ is unstable, and that with $n_r = 0$ and $n_i \neq 0$ is stable against small perturbations.

Finally, the IE factor, $f(t) = n_i(t)/n_i(0)$, evolves as

$$f(t) = \frac{1 + N' n_r(0)/n_i(0)}{1 + N' n_r(0)/n_i(0) e^{-K(N' n_r(0) + n_i(0))t}}$$

and the eventual ice enhancement reaches the maximum $f = 1 + N' n_r(0)/n_i(0)$ as $t \to \infty$.

b. Perturbation Analysis

A particular interest here is how the ice–number evolution is modified by slightly modifying its value by n'_{i*}. As a result, the rain–water number is also perturbed by, say, n'_{r*}. In this isolated setting, the total number density is conserved, thus we may set

$$n'_{r*} = -n'_{i*}. \tag{3.7}$$

The pertubation equation for n'_{i*} is given by

$$\dot{n}'_{i*} = \hat{K}(n_{i*}n'_{r*} + n_{r*}n'_{i*})$$

or by substituting the number–concentration constraint (3.7),

$$\dot{n}'_{i*} = \lambda n'_{i*},$$

where

$$\lambda = \hat{K}(n_{r*} - n_{i*}) \tag{3.8}$$

may be considered a feedback parameter characterizing this perturbation evolution. We see that at the initial stage when the rain–water is relatively abundant, $n_{r*} - n_{i*} > 0$, and the feedback is positive (splintering feedback), whereas when the ice number has substantially multiplied, $n_{r*} - n_{i*} < 0$, and the feedback becomes negative (drop–depletion feedback)

For any system in general, a feedback parameter may be defined as the rate of change of a forcing, Q, of system evolution with respect to its response (a change in its state variable, x) with $\lambda = dQ/dx$. Here, $\lambda > 0$ for a net positive feedback and $\lambda < 0$ for a net negative feedback. The forcing may be a function of variables quantifying several processes ($Q = Q(x, X_1, X_2, ...X_n)$). By performing this derivative as a partial derivative with respect to only one process variable, then the derivative quantifies the feedback from that process ($\lambda_i = (\partial Q/\partial X_i)(dX_i/dx)$). The total feedback parameter is the sum of partial derivatives corresponding to all the processes by the chain rule:

$\lambda = \sum_i \lambda_i$. Thus the net feedback parameter has contributions from all the positive and negative feedbacks of the system.

One can regard the above evolution equation ($\dot{n}_{i*} = \hat{K} n_{r*} n_{i*}$) for ice crystal number as arising from two separate processes: splintering of freezing drops, controlled by n_{r*}, and depletion of drops by collision with crystals, controlled by n_{i*}. The evolution equation of the system (Eq. 3.8) may be viewed as a special case of a more general equation, $\dot{n}_{i*} = Q$ where $Q = Q(n_{i*}, n_{r*})$, with rain and ice concentrations being hypothetically 'independent' contributions to the forcing Q causing a response in ice concentration. The feedback strength has contributions from both processes: $\lambda = dQ/dn_{i*} = \partial Q/\partial n_{i*} + \partial Q/\partial n_{r*} dn_{r*}/dn_{i*} = \lambda_1 + \lambda_2$ and with dn_{r*}/dn_{i*} expressing the linkage between rain and ice concentrations by the evolution equation for the drop depletion process. Considering $Q = \hat{K} n_{r*} n_{i*}$, the feedback parameter thus has the two contributions, $\lambda_1 = \partial Q/\partial n_{i*} = \hat{K} n_{r*} > 0$ measuring the feedback from splintering (a positive feedback) and $\lambda_2 = \partial Q/\partial n_{r*} dn_{r*}/dn_{i*} = \hat{K} n_{i*} \times (-1) < 0$ measuring the feedback from drop depletion (a negative feedback). Thus, we arrive again at the same equation as above, $\lambda = \lambda_1 + \lambda_2 = \hat{K}(n_{r*} - n_{i*})$.

The identified characteristics of the system is summarized in the phase-space of (n_{r*}, n_{i*}) in Fig. 2. Positive and negative feedbacks ($\lambda > 0$ and $\lambda < 0$) are realized over the regions of instability and stability (separated by the thick line, $n_{i*} = n_{r*}$), where splintering and drop-depletion feedbacks prevail respectively. The system travels along the trajectory (line with arrow, in which $n_{r*} + n_{i*} = n_0$) from one equilibrium point that is unstable ($n_{r*} = n_0$) to the other that is stable ($n_{i*} = n_0$). While travelling along the trajectory, the system goes from the realm of instability ($n_{r*} > n_{i*}$) to that of stability ($n_{r*} < n_{i*}$).

4. General Analysis

When the general case with $\hat{c}_0 \neq 0$, $\hat{c}_i \neq 0$, $\varepsilon_s \neq 0$ is considered, a full analytical solution is no longer available, thus various asymptotic expansion methods are called for.

a. Feedback Analysis

Probably the most useful starting point is to note that both the supercooled–drop and ice–particle number densities, n_{r*} and n_{i*}, can evolve independently in absence of the drop freezing and the subsequent ice fragmentation. We may consider this as a leading–order behaviour of the system (Eq 2.4) by setting $\hat{K} = 0$:

$$n_{r*}^{(0)} = (n_{r*}(0) - \frac{\hat{c}_0}{\varepsilon_s})e^{-\varepsilon_s t_*} + \frac{\hat{c}_0}{\varepsilon_s}, \tag{4.1a}$$

$$n_{i*}^{(0)} = n_{i*}(0) + \hat{c}_i t_*. \tag{4.1b}$$

The ice–fragmentation process is introduced as a process at $O(\hat{K})$. Here, taking $\hat{K}$ as a perturbation parameter for the asymptotic expansion is merely a device for analytically inferring the behavior of the system. Recall that in fact, $\hat{K} = 1$ by definition. However, in this manner, we can investigate how the evolution of the system is modified in the presence of ice fragmentation. Physically, this amounts for investigating the feedback to the system due to a presence of ice fragmentation.

Thus, a full solution may be approximately obtained by adding an $O(\hat{K})$–contribution to the above leading–order solution:

$$n_{r*} = n_{r*}^{(0)} + \hat{K} n_{r*}^{(1)}, \tag{4.2a}$$

$$n_{i*} = n_{i*}^{(0)} + \hat{K} n_{i*}^{(1)}. \tag{4.2b}$$

The $O(\hat{K})$–equations are given by

$$\dot{n}_{r*}^{(1)} = -n_{r*}^{(0)} n_{i*}^{(0)} - \varepsilon_s n_{r*}^{(1)}, \tag{4.3a}$$

$$\dot{n}_{i*}^{(1)} = n_{r*}^{(0)} n_{i*}^{(0)}. \tag{4.3b}$$

Here, note that the first term, $n_{r*}^{(0)} n_{i*}^{(0)}$, in the left–hand side of both equations represents the feedback to the system due to the ice–fragmentation process. It may also be important to note that this

term is nonlinear, but sicne this term is given, the above equations can readily be transformed into an integral form

$$n_{r*}^{(1)} = -e^{-\varepsilon_s t_*} \int_0^{t_*} n_{r*}^{(0)} n_{i*}^{(0)} e^{\varepsilon_s t} dt_*, \tag{4.4a}$$

$$n_{i*}^{(1)} = \int_0^{t_*} n_{r*}^{(0)} n_{i*}^{(0)} dt. \tag{4.4b}$$

By substituting the leading–order solutions (4.1a, b) into the above, and performing the integrals, we obtain

$$\begin{aligned} n_{r*}^{(1)} &= [\frac{\hat{c}_0}{\varepsilon_s^2}(n_{i*}(0) - \frac{\hat{c}_i}{\varepsilon_s}) - (n_{r*}(0) - \frac{\hat{c}_0}{\varepsilon_s})(n_{i*}(0)t_* + \frac{\hat{c}_i}{2}t_*^2)]e^{-\varepsilon_s t_*} \\ &\quad - \frac{\hat{c}_0}{\varepsilon_s^2}[(n_{i*}(0) - \frac{\hat{c}_i}{\varepsilon_s}) + \hat{c}_i t_*], \end{aligned} \tag{4.5a}$$

$$\begin{aligned} n_{i*}^{(1)} &= (n_{r*}(0) - \frac{\hat{c}_0}{\varepsilon_s})\frac{n_{i*}(0)}{\varepsilon_s}(1 - e^{-\varepsilon_s t_*}) \\ &\quad + \frac{\hat{c}_i}{\varepsilon_s}(n_{r*}(0) - \frac{\hat{c}_0}{\varepsilon_s})[\frac{1}{\varepsilon_s} - (\frac{1}{\varepsilon_s} + t_*)e^{-\varepsilon_s t_*}] + \frac{\hat{c}_0}{\varepsilon_s}(n_{i*}(0)t_* + \frac{\hat{c}_i}{2}t_*^2). \end{aligned} \tag{4.5b}$$

We see that apart from the exponentially decaying tendency associated with the sedimentation, the feedback is merely algebraic with no obvious destabilization tendency to the system.

The solutions may be further simplified by setting the initial condition to $n_{r*}(0) = \hat{c}_0/\varepsilon_s$ and $n_{i*}(0) = 0$:

$$n_{r*}^{(1)} = -\frac{\hat{c}_0\hat{c}_i}{\varepsilon_s^2}[\frac{1}{\varepsilon_s}(e^{-\varepsilon_s t_*} - 1) + t_*], \tag{4.6a}$$

$$n_{i*}^{(1)} = \frac{1}{2}\frac{\hat{c}_i\hat{c}_0}{\varepsilon_s}t_*^2. \tag{4.6b}$$

The solution by this feedback analysis would be indicative of the evolution of the system at onset of ice fragmentation. Note that the solution for n_{r*} may further be approximated to

$$n_{r*}^{(1)} \simeq -\frac{1}{2}\frac{\hat{c}_i\hat{c}_0}{\varepsilon_s}t_*^2 \tag{4.7}$$

to the limit of $t \to 0$. We see that the dimensionless concentrations of rain water and ice crystals decrease and increase at the same rate, initially. This is consistent with the splintering positive

feedback of ice multiplication (noted above for the simplest system) being boosted by the rates of primary generation of crystals and drops, as well as by the fall-out time of drops being long (compared to the characteristic time for glaciation). Fall-out of drops has a damping effect on the splintering positive feedback.

b. Taylor–Expansion Solution

The feedback analysis of the last subsection suggests that the initial tendency of the system due to the ice fragmentation is merely algebraic. It further suggests that an exact initial tendency of the system may be obtained by directly applying the Taylor expansion to the solution. Thus, we set

$$n_{r*} = \sum_{j=0}^{\infty} n_{r*,j} t_*^j, \tag{4.8a}$$

$$n_{i*} = \sum_{j=0}^{\infty} n_{i*,j} t_*^j. \tag{4.8b}$$

In substitution of these Taylor expansions into the original full equations (2.4a, b) leads to a solution. In deriving the solution, we note particularly

$$n_{r*} n_{i*} = \sum_{j=0}^{\infty} \left[\sum_{l=0}^{j} n_{r*,l} n_{i*,j-l} \right] t_*^j.$$

With $j = 0$, we obtain

$$n_{r*,1} = \hat{c}_0 - \hat{K} n_{r*,0} n_{i*,0} - \varepsilon_s n_{r*,0}, \tag{4.9a}$$

$$n_{i*,1} = \hat{c}_i + \hat{K} n_{r*,0} n_{i*,0}. \tag{4.9b}$$

Here, $n_{r*,0}$ and $n_{i*,0}$ are defined by the initial conditions. With $j = 1$, we further obtain

$$n_{r*,2} = -\hat{K}(n_{r*,0} n_{i*,1} + n_{r*,1} n_{i*,0}) - \varepsilon_s n_{r*,1}, \tag{4.10a}$$

$$n_{i*,2} = \hat{K}(n_{r*,0} n_{i*,1} + n_{r*,1} n_{i*,0}). \tag{4.10b}$$

In order to simplify the expressions, again, we set $n_{r*,0} = \hat{c}_0/\varepsilon_s$ and $n_{i*,0} = 0$. Then we obtain

$$n_{r*,1} = 0,$$

$$n_{i*,1} = \hat{c}_i,$$

$$n_{r*,2} = -\hat{K}\frac{\hat{c}_i\hat{c}_0}{\varepsilon_s},$$

$$n_{i*,2} = \hat{K}\frac{\hat{c}_i\hat{c}_0}{\varepsilon_s}.$$

Putting them together, the initial tendency of the solution is given by

$$n_{r*} = \frac{\hat{c}_0}{\varepsilon_s}(1 - \hat{K}\hat{c}_i t_*^2) + \cdots, \tag{4.11a}$$

$$n_{i*} = \hat{c}_i(t_* + \frac{\hat{K}\hat{c}_0}{\varepsilon_s}t_*^2) + \cdots. \tag{4.11b}$$

This solution (4.11a, b) may be compared with (4.7) and (4.6b) obtained in the last subsection. We see that the feedback analysis underestimates the effect of the ice fragmentation by half due to its perturbation treatment.

c. Feedback Analysis with Distorted Physics

A variation to the feedback analysis in Sec. 4.*a* is to differentiate the strength of the ice freezing–fragmentation to the hydrometeor types. Thus, we re–write Eqs. (2.4a, b) as

$$\dot{n}_{r*} = \hat{c}_0 - \hat{K}_1 n_{i*} n_{r*} - \varepsilon_s n_{r*}, \tag{4.12a}$$

$$\dot{n}_{i*} = \hat{c}_i + \hat{K}_2 n_{r*} n_{i*}. \tag{4.12b}$$

Here, we may artificially assume that the freezing fragmentation is negligible for the supercooled drops, thus $\hat{K}_1 \ll 1$, and the effect of freezing–fragmentation is only felt by the ice particles to the leading order, assuming $\hat{K}_2 = O(1)$. Thus, we solve the problem with the following asymptotic

expansion:

$$n_{r*} = n_{r*}^{(0)} + \hat{K}_1 n_{r*}^{(1)} + \cdots$$

$$n_{i*} = n_{i*}^{(0)} + \hat{K}_1 n_{i*}^{(1)} + \cdots$$

Though such an assumption is hardly justified from a physical basis, this procedure provides a useful insight into the evolution of the system during ice fragmentation. For this reason, we shall call this method the *feedback analysis with distorted physics*.

The leading–order solution for n_{r*} is, thus, given by Eq. (4.1a), whereas we solve the full problem for n_{i0*} to the leading order:

$$(\frac{d}{dt_*} - \hat{K}_2 n_{r*}^{(0)}) n_{i*}^{(0)} = \hat{c}_{i*}$$

This equation is linear in respect to $n_{i*}^{(0)}$, and its solution can easily be written in an integral form:

$$n_{i*}^{(0)} = [n_{i*}(0) + \int_0^{t_*} \hat{c}_i \exp(-\int_0^{t'_*} \hat{K}_2 n_{r*}^{(0)} dt''_*) dt'_*] \exp(\hat{K}_2 \int_0^{t_*} n_{r*}^{(0)} dt_*)$$

The second integral is readily performed and we obtain

$$\int_0^{t_*} n_{r*}^{(0)} dt_* = \frac{1}{\varepsilon_s}(n_{r*}(0) - \frac{\hat{c}_0}{\varepsilon_s})(1 - e^{-\varepsilon_s t_*}) + \frac{\hat{c}_0}{\varepsilon_s} t_*$$

However, the first integral

$$\int_0^{t_*} \exp(-\hat{K}_2 \int_0^{t'_*} n_{r*}^{(0)} dt''_*) dt_* = \int_0^{t_*} \exp[-\frac{\hat{K}_2}{\varepsilon_s}(n_{r*}^{(0)}(0) - \frac{\hat{c}_0}{\varepsilon_s})(1 - e^{-\varepsilon_s t_*}) - \frac{\hat{K}_2 \hat{c}_0}{\varepsilon_s} t_*] dt_*$$

is not readily integrable, thus we focus on the two limits, $t_* \sim 0$ and $t_* \to \infty$.

(i) When $t_* \sim 0$, noting $1 - e^{-\varepsilon_s t_*} \simeq \varepsilon_s t_*$, the integral becomes

$$\int_0^{t_*} \exp(-\hat{K}_2 \int_0^{t'_*} n_{r*}^{(0)} dt''_*) dt_* \simeq \frac{1}{\hat{K}_2 n_{r*}^{(0)}(0)}(1 - e^{-\hat{K}_2 n_{r*}^{(0)}(0) t_*}),$$

and the solution is

$$n_{i*}^{(0)} \simeq (n_{i*}^{(0)}(0) + \frac{\hat{c}_i}{\hat{k}_2 n_{r*}^{(0)}(0)}) e^{\hat{K}_2 n_{r*}^{(0)}(0) t} - \frac{\hat{c}_i}{\hat{k}_2 n_{r*}^{(0)}(0)}. \tag{4.13a}$$

(ii) When $t_* \to \infty$, the integral asymptotically approaches to:

$$\int_0^{t_*} \exp(-\hat{K}_2 \int_0^{t'_*} n_{r*}^{(0)} dt''_*) dt_* \to -\frac{\varepsilon_s}{\hat{K}_2 \hat{c}_0} \exp[-\frac{\hat{K}_2}{\varepsilon_s}(n_{r*}^{(0)}(0) - \frac{\hat{c}_0}{\varepsilon_s}) - \frac{\hat{K}_2 \hat{c}_0}{\varepsilon_s} t_*] + \frac{1}{\hat{K}_2 n_{r*}^{(0)}(0)},$$

thus

$$n_{i*}^{(0)} \to (n_{i*}^{(0)}(0) + \frac{\hat{c}_i}{\hat{K}_2 n_{r*}^{(0)}(0)}) \exp[\frac{\hat{K}_2}{\varepsilon_s}(n_{r*}^{(0)}(0) - \frac{\hat{c}_0}{\varepsilon_s}) + \frac{\hat{K}_2 \hat{c}_0}{\varepsilon_s} t_*] - \frac{\varepsilon_s \hat{c}_i}{\hat{K}_2 \hat{c}_0}. \tag{4.13b}$$

It is seen that in both limits, the ice–crystal number increases exponentially with time when the decrease of supercooled drops by freezing is neglected.

We now turn to $O(\hat{K}_1)$ in order to see the modifications of the both particles numbers by the exponential ice–fragmentational multiplication:

$$(\frac{d}{dt_*} + \varepsilon_s) n_{r*}^{(1)} = -n_{r*}^{(0)} n_{i*}^{(0)}, \tag{4.14a}$$

$$(\frac{d}{dt_*} - \frac{\hat{K}_2}{\hat{K}_1} n_{r*}^{(0)}) n_{i*}^{(1)} = \frac{\hat{K}_2}{\hat{K}_1} n_{r*}^{(1)} n_{i*}^{(0)}. \tag{4.14b}$$

Though it is possible to explicitly write down the full asymptotic solutions for the same two limits as considered for the leading order, the expressions are lengthy, and not particularly illuminating. For this reason, we focus on the case with $n_{r*}(0) = \hat{c}_0/\varepsilon_s$ and $n_{i*}(0) = 0$. Note that coincidentally, in this case, the two leading–order solutions (4.13a, b) agree. We also focus only on the most dominant exponential term in the solution of Eqs. (4.14a, b), neglecting the various exponentially–decaying terms that follow.

After these simplifications, the first–order modification to the supercooled rain density, n_{r*}, due to the freezing is given by:

$$n_{r*}^{(1)} = -\frac{\varepsilon_s \hat{c}_i}{\hat{K}_2(\hat{K}_2 \hat{c}_0 + \varepsilon_s^2)} e^{(\hat{K}_2 \hat{c}_0/\varepsilon_s) t_*} + \cdots \tag{4.15a}$$

The result shows that as the first–order effect, collision freezing exponentially depletes the supercooled water due to the exponential multiplication of ice. If this result is taken literally, the supercooled water would be completely depleted over a finite time. In reality, as the supercooled

water begins to deplete, the ice fragmentation also slows down, thus it is more likely that supercooled water will be depleted in slower rate.

In turn, the first–order modification to the ice–particle number is:

$$n_{i*}^{(1)} = -\frac{\hat{c}_0\hat{c}_i}{\hat{K}_2\hat{c}_0+\varepsilon_s^2}\left[\frac{\hat{K}_2^2\hat{c}_0^2+\varepsilon_s^2\hat{K}_2\hat{c}_0+\varepsilon_s^4}{\varepsilon_s\hat{K}_2\hat{c}_0(\hat{K}_2\hat{c}_0+\varepsilon_s^2)}+\frac{\hat{c}_0\hat{c}_i}{\hat{K}_2\hat{c}_0+\varepsilon_s^2}t_*\right]e^{\hat{K}_2 n_{r*}^{(0)}(0)t_*}+\cdots \tag{4.15b}$$

We see the exponential ice multiplication tendency is first, suppressed by the constant factor (the first term), and further decreases linearly with time (the second term). Thus, the dominant exponential term becomes negative over a finite term, and the only remaining positive contributions are neglected exponentially–decaying terms. We interpret that the result suggests that though the ice multiplies with time, the growth is weaker than exponential.

d. Asymptotic Tendency towards $t_* \to \infty$

The analysis of the last subsection suggests (though it does not show) that the supercooled water would deplete with a rate slower than exponential, and also the ice multiplies by fragmentation with a rate slower than exponential. The most likely case is that the supercooled water decreases, and the ice particles increase both algebraically with time. Thus, to the asymptotic limit towards $t_* \to \infty$, we may set

$$n_{r*} \sim n_{r*0}t_*^{-\alpha}, \tag{4.16a}$$

$$n_{i*} \sim n_{i*0}t_*^{\beta}. \tag{4.16b}$$

Here, both α and β are expected to be positive constants, and the symbol $\sim$ suggests that we are only concerned with the asymptotic tendency toward $t_* \to \infty$.

Substitution of the asymptotic expressions (4.16a, b) into Eqs. (2.4a, b) leads to

$$-\alpha n_{r*0}t_*^{-(\alpha+1)} \sim \hat{c}_0 - \hat{K}n_{i*0}n_{r*0}t_*^{-\alpha+\beta} - \varepsilon_s n_{r*0}t_*^{-\alpha}, \tag{4.17a}$$

$$\beta n_{i*0}t_*^{\beta-1} \sim \hat{c}_{i*} + \hat{K}n_{r*0}n_{i*0}t_*^{-\alpha+\beta}. \tag{4.17b}$$

In order this asymptotic expression to be valid, the most dominant terms in terms of the power in t_* must balance.

In Eq. (4.17a), we find $t_*^{-(\alpha+1)} \ll t_*^{-\alpha} \ll t_*^{-\alpha+\beta}$, thus the dominant expected asymptotic balance is:

$$\hat{c}_0 - \hat{K} n_{i*0} n_{r*0} t_*^{-\alpha+\beta} \sim 0. \tag{4.18}$$

This balance is achieved when $-\alpha+\beta = 0$, or $\alpha = \beta$. It may be important to note that in asymptotic limit of $t_* \to \infty$, the equation for the supercooled rain number becomes quasi–stationary (*i.e.,* the temporal tendency in the left hand side does not contribute to the leading order), and also the sedimentation no longer plays a leading role (*i.e.,* the 3rd term is the right hand side does not contribute to the leading order).

By substituting $\alpha = \beta$ into Eq. (4.17b), we find

$$\beta n_{i*0} t_*^{\beta-1} \sim \hat{c}_{i*} + \hat{K} n_{r*0} n_{i*0}.$$

Since the right hand side is positive definite, it must be balanced by a constant growing tendency of the ice number, thus

$$\beta = 1,$$

and also $\alpha = 1$ as a result.

Constants, n_{r*0} and n_{i*0}, may be determined in a more straightforward manner by considering the conservation of the total particle number, which is obtained by taking the sum of Eqs. (2.4a, b):

$$\frac{d}{dt_*}(n_{r*} + n_{i*}) = \hat{c}_0 + \hat{c}_i - \varepsilon n_{r*}.$$

As $t_* \to \infty$, $n_{r*} \to 0$, thus the above conservation law asymptotically approaches to

$$\dot{n}_{i*} \sim \hat{c}_0 + \hat{c}_i. \tag{4.19}$$

Substituting Eq. (4.16a) into Eq. (4.19) with $\beta = 1$, we immediately obtain $n_{i*0} = \hat{c}_0 + \hat{c}_i$. By further substituting this result into Eq. (4.18), we find $n_{r*0} = \hat{c}_0[\hat{K}(\hat{c}_0 + \hat{c}_i)]^{-1}$ Thus, the asymptotic solution towards $t \to \infty$ becomes

$$n_{r*} \sim \frac{\hat{c}_0}{\hat{K}(\hat{c}_0 + \hat{c}_i)} t_*^{-1}, \tag{4.20a}$$

$$n_{i*} \sim (\hat{c}_0 + \hat{c}_i) t_*. \tag{4.20b}$$

In the limit of the long time scale, the ice crystals multiply by fragmentation linearly with time at a rate defined by the sum of the supercooled–drop and primary–ice sources.

Finally, the asymptotic solution becomes when dimensions are included:

$$n_r \sim \frac{c_0}{\hat{K}K(N'c_0 + c_i)} t^{-1}, \tag{4.20a}$$

$$n_i \sim (N'c_0 + c_i) t. \tag{4.20b}$$

The definition of IE ratio, $f \equiv n_i*(t*)/n_i*^{(0)}(t*)$, is the ratio of the total ice concentration to the primary ice concentration. Thus it is a measure of the extent of secondary ice production.

So in the general case, if $\hat{c}_i$ is non-zero and $t \to \infty$:

$$f = (N'c_0/c_i + 1)/(n_i(t=0)/(tc_i) + 1) \to 1 + N'c_0/c_i \tag{1}$$

The maximum IE ratio is approached on a timescale of $n_i(t=0)/c_i$.

Otherwise without continuous primary ice nucleation, $\hat{c}_i = 0$ implies:

$$f(t) \to N'c_0 t/(n_i(t=0))$$

taking the dimensional expressions for the source terms. Now there is no upper limit on the IE ratio, and it increases with time at a constant rate of $N'c_0/n_i(t=0)$.

The supercooled–drop number decreases only weakly with time at a rate $\sim t_*^{-1}$ maintaining a quasi–stationarity with the generation rate balancing with the collision freezing rate. The rain sedimentation does not play a leading role.

e. Perturbation Analysis

Finally, the perturbation analysis considered in Sec. 3.*b* may also be performed for the full problem. However, the procedure is more involved with the fact that the source and the sink terms are involved in the full system, thus the total number density is no longer conserved, and it is no longer possible to invoke a simple constraint as Eq. (3.7). Instead, we have to consider explicitly the two perturbation equations for both n'_{r*} and n'_{i*}:

$$\dot{n}'_{r*} = -(\hat{K}n_{i*} + \varepsilon_s)n'_{r*} - \hat{K}n_{r*}n'_{i*}, \tag{4.21a}$$

$$\dot{n}'_{i*} = \hat{K}(n_{i*}n'_{r*} + n_{r*}n'_{i*}). \tag{4.21b}$$

The analysis of this system is further involved due to the fact that the linear operator in the right–hand side also evolves with time. However, the problem can be simplified, as implicitly assumed in Sec. 3.*b*, when the evolution of the reference state, (n_{r*}, n_{i*}), is considered much slower than that of the perturbations. In this case, the time derivative in the left–hand side may be replaced by an eigenvalue, λ, and the above problem reduces to that of finding the eigenvalues for the linear operator in the right hand side, which is determined from

$$\lambda^2 - (\hat{K}n_{r*} - \hat{K}n_{i*} - \varepsilon_s)\lambda + \hat{K}^2 n_{i*}n_{r*} - (\hat{K}n_{i*} + \varepsilon_s)\hat{K}n_{r*} = 0.$$

Solving it for λ, we obtain the two eigenvalues (adding the subscripts 1 and 2 for distinction):

$$\lambda_1 = \frac{(\hat{K}n_{r*} - \hat{K}n_{i*} - \varepsilon_s)}{2}[1 + \{1 + \frac{4\varepsilon_s\hat{K}n_{r*}}{(\hat{K}n_{r*} - \hat{K}n_{i*} - \varepsilon_s)^2}\}^{1/2}],$$

$$\lambda_2 = \frac{(\hat{K}n_{r*} - \hat{K}n_{i*} - \varepsilon_s)}{2}[1 - \{1 + \frac{4\varepsilon_s\hat{K}n_{r*}}{(\hat{K}n_{r*} - \hat{K}n_{i*} - \varepsilon_s)^2}\}^{1/2}].$$

The first eigenvalue reduces to Eq. (3.8) in the limit of $\varepsilon_s \to 0$, whereas the second reduces to $\lambda_2 = 0$. The latter is simply interpreted as a manifestation of the conservation of the total particle number number (3.7).

When a finite sedimentation rate ($\varepsilon_s \neq 0$) is considered, the threshold from the positive to negative feedback for λ_1 reduces by ε_s (*i.e.*, bias towards a negative "feedback"). Thus, the neutral line shifts from $n_{i*} = n_{r*}$ to $n_{i*} = n_{r*} - \varepsilon_s$: the critical ice number density becomes smaller in the presence of sedimentation. Some examples of the neutral lines are plotted in Fig. 3a for selective sedimentation rates, ε_s. In the presence of sedimentation, however, the neutral line no longer separates between the stable and the unstable regimes, but the stable regime upper left of the neutral line identified in Fig. 2 also destabilizes due to the second eigenvalue, λ_2. Most importantly, in these general situations, the perturbation evolution of the system is no longer interpreted in terms of a single "perturbation" parameter, but the actual perturbation evolution is determined by a linear combination of two exponential tendencies characterized by two eigenvalues, sensitively depending on the initial perturbation. Trajectories in the phase-space are shown in Fig. 3a for the special case of $\varepsilon_s = 0$ and $\hat{c}_i = 0$ by numerical integration of Eq (2.4), with primary ice only implicitly represented by an initial nonzero value of ice concentration, $n_{i*}(t* = 0) = 0.001$. The simulations are integrated until $t* = 10^3$.

The evolution over time of the IE ratio, f, for the same trajectories is shown in Fig. 3b. Two stages of the glaciation are evident. First, there is the usual exponential growth of the ice concentration by an IE ratio of up to 10^3 in a dimensionless time of $t* <$ 1-10. During this stage, the rain concentration is depleted almost to zero. If the integration of the corresponding dimensional equations were performed, this initial stage would correspond to the time-scale of explosive fragmentation noted above of $\tau = 1/(K(n_i(0) + n_r(0)N'))$. Second, there is the subsequent exponential relaxation to the asymptotic solution when $t* >$ 1-10, coinciding with a balance between supply

of fresh drops ($\hat{c}_0 > 0$) and their depletion by fragmentation and collisions with ice splinters. In this second stage, the rain concentration decreases steadily, inversely proportional with time.

5. Discussions

a. Efficiency of the Ice Multiplication Processes

Our theoretical investigation reveals that the ice multiplication by fragmentation of the freezing drops is not always as potentially effective as the two other ice multiplication processes examined by Yano and Phillips (2011), and Yano *et al.* (2016): Hallett–Mossop and ice–ice collision processes. As shown in the Appendix C of Yano and Phillips (2011), the ice multiplication rate by the Hallett–Mossop process is linearly proportional to the existing graupel number density. This leads to an exponential multiplication of ice with time, assuming that the system is in quasi–equilibrium between the ice particles and graupel, and also the supercooled cloud–droplets are re–adjusted to an equilibrium number as graupel sweeps them through as the latter falls. As carefully analyzed in Yano *et al.* (2011: see the Appendix especially), the ice multiplication by ice–ice collision is fundamentally nonlinear, being proportional to the square of the ice–number density. In the idealized state with infinite water–vapor supply, this leads to an explosive increase of the ice number to infinity within a finite time.

Compared to those rather strong multiplication tendencies found with these two processes, the ice multiplication by fragmentation of freezing drops often tends to be rather modest. This stems from the fact that this process relies on a number of supercooled drops available in the system, and it essentially limits the possible number of ice fragments that can be generated. When the ice fragmentation by freezing drops is considered in its isolation, as in Sec. 3, this conclusion is especially clear: the final total number of ice fragments found is simply $N' n_r(0) + n_i(0)$ with $N = N' + 1$ the number of secondary ice fragments generated per freezing collision, and $n_r(0)$, $n_i(0)$ are the initial numbers of supercooled drops and ice crystals, respectively.

When both supercooled–water rain and primary–ice sources are added to the system, as in Sec. 4, the behavior of the system becomes more involved. However, in the limit of the long time–scale, the ice fragmentation number simply increases linearly with time by the rate that both supercooled water and primary ice are supplied. We see that such a multiplication tendency is, generally, much weaker than any of those found in Hallett–Mossop or ice–ice collision process.

However, in some observational situations, fragmentation of freezing drops *does* become a primary process of ice multiplication, especially when there is copious supercooled rain initially and temperatures are optimal. A case during the ICET is such an example.

b. Comparison with the Observation

A quantitative observational comparison with the present theoretical results is provided by Lawson *et al.* (2015), who present the measurements during ICET over U.S. Virgin Islands in July 2011. Their flights measuring cloud properties were performed in ascending order so that a Lagrangian interpretation of data following the convective updrafts can be developed. The Lagrangian interpretation would also be further facilitated by considering the ice–fragmentation process in its isolation as in Sec. 3.

In this framework, the key conserved quantity is the total particle number with the supercooled drops multiplied by the fragmentation number per collision freezing. It also follows that the total water content, as a sum of liquid and ice, is also conserved. Hence, the scatter plots for liquid and ice values, both in terms of the number density and the water content would form a linear line with a negative slope. The scatter plots using the measurements for varying heights (temperature levels) averaged over various convective cores for both quantities in Fig. 4 clearly present a negative correlation both for the number density (a) and the water content (b), being consistent with the theory presented in Sec. 3, though the distributions are hardly aligned to any line.

The strong scatter may be understood by two reasons: 1) the plots are hardly form a single convective event, but a collection of many convective cores, though all of them are in similar regime; 2) the source and the loss terms for both liquid and ice, neglected in the theory, would not be negligible in practice. Considering those two caveats, these two scatter plots would rather be considered a good support for the idealized theory presented in Sec. 3.

A rather surprising result from their data analysis is a fast glaciation process: they found that 3–5 g m^{-3} supercooled liquid are almost all glaciated over 3 min time at an elevation of 1–1.5 km higher within an updraft core. Here, this rapid glaciation rate is easily explained by the theoretical analysis in Sec. 3. Note that the collision efficiency is defined by

$$K = \pi r_d^2 v_T$$

in terms of the radius, r_d, of the supercooled drops, and the differential vertical velocity, v_T, between the supercooled drops and ice crystals. Assuming, $r_d \sim 10^2$ μm$\sim 10^{-4}$ m, $v_T \sim 1$ m/s, we obtain

$$K \sim r_d^2 v_T \sim 10^{-8}\,\mathrm{m}^3/\mathrm{s}$$

Also setting $n_r \sim 1$ cm$^{-3} \sim 10^6$ m^{-3}, $N' \sim 1$, the characteristic glaciation rate is estimated by

$$N' K n_r \sim 10^{-1}\,1/\mathrm{s},$$

and the characteristic time scale is $\tau \sim 10$ sec by following the definition (3.5). Noting from Fig. 1 that it typically takes about ten characteristic time scales for completing the glaciation, a time required for completing the glaciation is also only 10^2 sec, being fairly comparable with the observational estimate of 3 min.

c. Asymptotic Expansion Approaches

The present study has employed various asymptotic–expansion methods in order to elucidate the basic behavior of the system for ice fragmentation by collision freezing of supercooled drops.

Here, we emphasize that not all the asymptotic solutions presented herein are equally useful. Some of them are not precise even in asymptotic sense, but merely for providing qualitative insights. Nevertheless, they help to identify more rigorous methods for deriving more precise solutions. For example, the feedback analysis in Sec. 4.*a* suggests the initial tendency of the system is algebraic in time, that further motivates us to determine the exact initial tendency by the Taylor expansion method (Sec. 4.*b*). Though the exact Taylor–expansion result demonstrates that the feedback analysis halves the initial parabolic tendency, at the same time, without support of the feedback analysis, the Taylor–expansion solution is justified only in a strong limit of $t \to 0$, because in general, the presence of an exponentially growing tendency invalidates the Taylor–expansion solution very rapidly in time. Another example is an approach of distorted physics considered in Sec. 4.*c*. Again, though this analysis is not quantitatively accurate, the result suggests to consider an algebraic tendency of the solution in the long time–scale limit, as considered in Sec. 4.*d*.

Asymptotic analyses presented herein are hardly exhaustive either, because some asymptotic analyses are not particularly illuminating. For example, it is possible to consider the modification of the solution presented in Sec. 3 by adding the sources, $\hat{c}_0$ and $\hat{c}_i$, as perturbation terms. However, such an analysis hardly elucidates a rather drastic change of the system behavior by adding finite sources, as considered in Sec. 4.

Some of the analyses turn out to be rather subtle. For example, an alternative feedback analysis by another assumption of distorted physics, $\hat{K}_2 \ll \hat{K}_1 \sim 1$, may also be considered. In this case, the system exponentially approaches new equilibrium states up to first order. Yet it is rather difficult to draw any physically meaningful conclusions from this solution.

d. Stochasticity of the Ice Fragmentation Process

Finally, we should keep in mind that the fragmentation number, N', of ice per collision freezing is not a fixed number even when a collision between a drop and an ice particle with fixed diameters

is considered. One reason is that the number of fragments per spherically frozen drop (mode 1) varies by orders of magnitude depending on temperature. Vertical motions due to sloped in-cloud drafts combined with sedimentation create variability of the ambient temperature. Equally, even for identical conditions of freezing temperature and drop size, the number of drop fragments varies dramatically from drop to drop. Macroscopically, it may be assumed to be probabilistic. Kolomeychuk *et al.* 1975 observed that about 10% of all drops in their experiment (1.6 mm) emitted about 90% of all the detected splinters. Considering only drops freezing between -15°C and -18°C, 90% of the splinters were from a third of the drops.

Details of the collision process are complex for the most purposes of cloud microphysical modeling, and the outcome of the fragmentation number by collision freezing may simply be considered a random number (*cf.,* Kolomeychuk *et al.* 1975). As a result, the ice fragmentation may be considered a stochastic process. This is an aspect, where further investigation may be warranted. Here, we present short general theoretical observations for facilitating further studies.

As a whole, the contribution of stochasticity would also be best understood by adding this component as a perturbation, say, $\delta N'$. In the general case considered in Sec. 4, under the asymptotic limit to the long time scale, the ice–particle number, n_i, asymptotically evolves solely depending on the strength of the two hydrometeor sources. This asymptotic tendency is not affected, even when the fragmentation number fluctuates randomly. The latter effect only affects the time evolution of the supercooled–drop number, n_r. It can be shown that the resulting fluctuation, n_r', is dictated by a Brownian motion induced by white noise, $\delta N'$, under a linear drag with a drag coefficient linearly increasing with time.

On the other hand, when the ice fragmentation process is considered in isolation, as in Sec. 3, we find that stochastic fluctuations, $\delta N'$, of fragmentation induce multiplicative noise. As found the

633 case for an analogous problem with ice–ice collision multiplication by Yano and Phillips (2016),
634 this multiplicative noise process may contribute to the whole system in a nontrivial manner.

635 *Acknowledgment.* The first author (VTJP) was supported by three research grants, from Swedish
636 Research Council for Sustainable Development (FORMAS; award number 2018-01795), Swedish
637 Research Council (VR; award number 2015-05104) and US Department of Energy Atmospheric
638 Sciences Research Program (award number: DE-SC0018932). The topics of these awards concern
639 mechanisms for ice production in clouds and their relation of aerosol conditions.

References

Auer, A. H., D. L. Veal, and J. D. Marwitz, 1969: Observations of ice crystal an dice nuclei concentrations in stable cap clouds. *J. Atmos. Sci.*, **26**, 1342–1343.

Brownscombe, J. L., and N. S. C. Thorndike, 1968: Freezing and shattering of water drop sin free fall. *Nature*, **220**, 687–689.

Dye, J. E., and P. V. Hobbs, 1968: The influence of environmental parameters on the freezing and fragmentation of suspended water drops. *J. Atmos. Sci.*, **25**, 82–96.

Hallett, J. and Mossop, S. C., 1974: Production of secondary ice particles during the riming process. Nature, 249, p. 2628

Hobbs, P. V., 1969: Ice multiplication in clouds. *J. Atmos. Sci.*, **26**, 315–318.

Hobbs, P. V., and A. J. Alkezweeny, 1968: The fragmentation of freezing water droplets in free fall. *J. Atmos. Sci.*, **25**, 881–888.

Kolomeychuk, R. J. , D. C. McKay, and J. V. Iribarne, 1975: The fragmentation and electrification of freezing drops. *J. Atmos. Sci.*, **32**, 974–979.

Latham, J., and B. J. Mason, 1961: Generation of electric charge associated with the formation of soft hail in thunderclouds. *Proc. R. Soc. Lond.*, **A 260**, 537–549. DOI: 10.1098/rspa.1961.0052.

Lawson, R. P., S. Woods, and H. Morrison, 2015: The microphysics of ice and precipitation development in tropical cumulus clouds. *J. Atmos. Sci.*, **72**, 2429–2445.

Mossop, S. C., 1970: Concentration of ice crystals in clouds. *Bull. Amer. Meteor. Soc.*, **51**, 474–479.

Phillips, V. T. J., A. M. Blyth, T. W. Choularton, P. R. A. Brown, J. Latham, 2001: The glaciation of a cumulus cloud over New Mexico. *Q. J. R. Meteorol. Soc.*, **127**, 1513–1534.

663Phillips, V. T. J., S. Patade, J. Gutierrez and A. Bansemer, 2018: Secondary ice production by
664 fragmentation of freezing of drops: formulation and theory. *J. Atmos. Sci.*, **75,** 3031–3070
665Pruppacher, H. R., and J. D. Klett, 1997: *Microphysics of Clouds and Precipitation, Second Re-*
666 *vised and Enlarged Edition with an Introduction to Cloud Chemistry and Cloud Electricity*,
667 Kluwer Academic Publisheres, Dordrecht, 954pp.
668Takahashi, C., and A. Yalashita, 1969: Deformation and fragmentation of freezing water drops in
669 free fall. *J. Met. Soc. Japan*, **47**, 431–436.
670Wildeman, S., S. Sterl, C. Sun, and D. Lohse, 2017: Fast dynamics of water droplets freezing from
671 the outside in. *Phys. Rev. Lett.*, **118**, 084101.
672Yano, J.-I., and V. T. J. Phillips, 2011: Ice-ice collisions: An ice multiplication process in atmo-
673 spheric clouds, *J. Atmos. Sci.*, **68**, 322–333.
674Yano, J.-I., and V. T. J. Phillips, 2016: Explosive ice multiplication induced by multiplicative–
675 noise fluctuation of mechanical break–up in ice-ice collisions. *J. Atmos Sci.*, **73**, 4685–4697.
676Yano, J.–I., V. T. J. Phillips and V. Kanawade, 2016: Explosive Ice Multiplication by Mechanical
677 Break-up in Ice-Ice Collisions: A Dynamical-System Based Study. *Quator. J. Roy. Meteor.*
678 *Soc.*,**142**, 867–879.

*LIST OF FIGURES

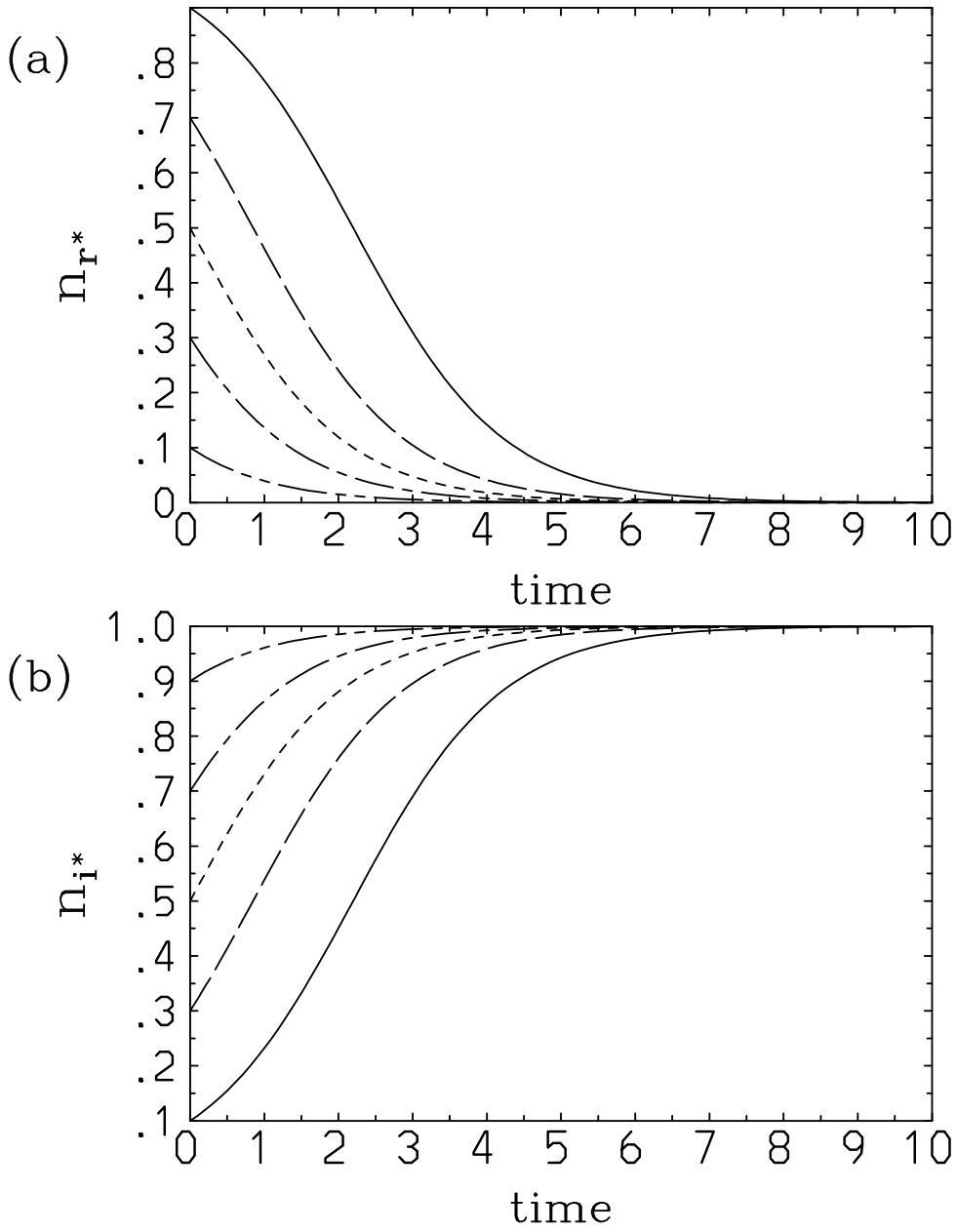

FIG. 1. Time evolution of the particle number densities with various initial conditions when the ice–fragmentation process is considered in its isolation: for (a) supercooled drops, n_{r*}, and (b) ice crystals, n_{i*}. All the variables are nondimensionalized as described in the text.

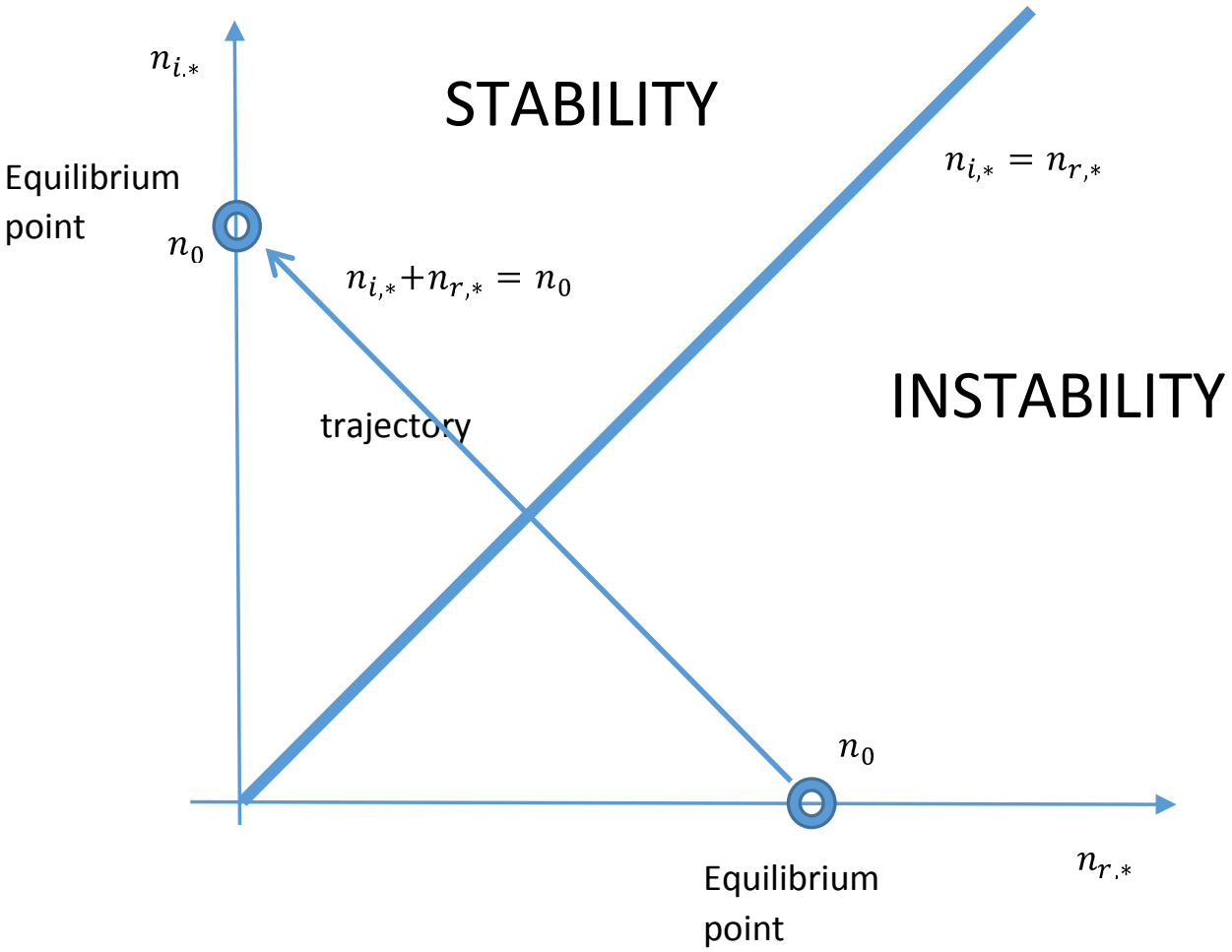

FIG. 2. The stability characteristics of the system when no source and sink is considered as in Sec. 3.

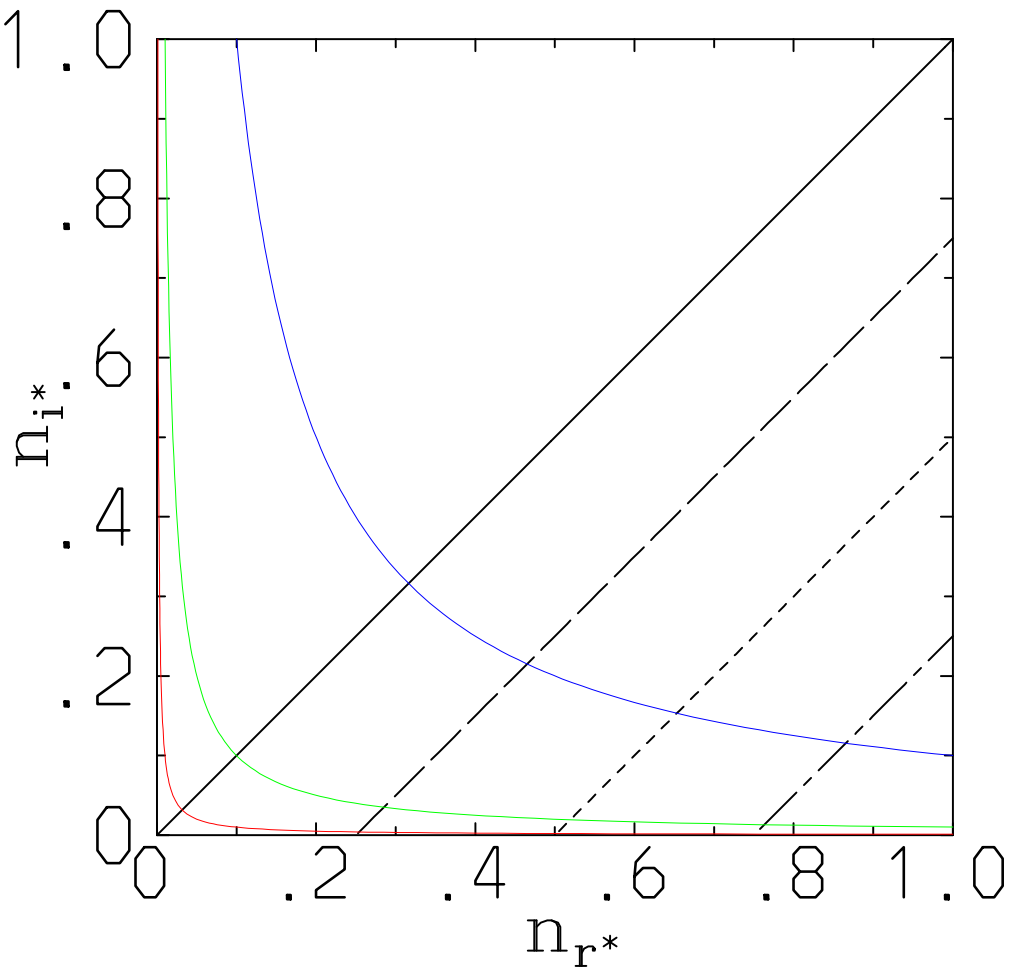

FIG. 3. The stability characteristics of the system in the general case: shown are the neutral lines with selective choice of the sedimentation rates: $\varepsilon_s = 0$ (solid), 0.25 (long dash), 0.5 (short dash), and 0.75 (chain dash). Note that in the general case, the system is unstable at both sides of the neutral line, with a weak instability to the upper left of the neutral line when the sedimentation effect is small. Some examples of trajectories are also shown based on the asymptotic solution (4.20) with $\hat{c}_0 = 10^{-1}$ (blue), 10^{-2} (green), and 10^{-3} (red): the system evolves in the direction of decreasing n_{r*} and increasing n_{i*}.

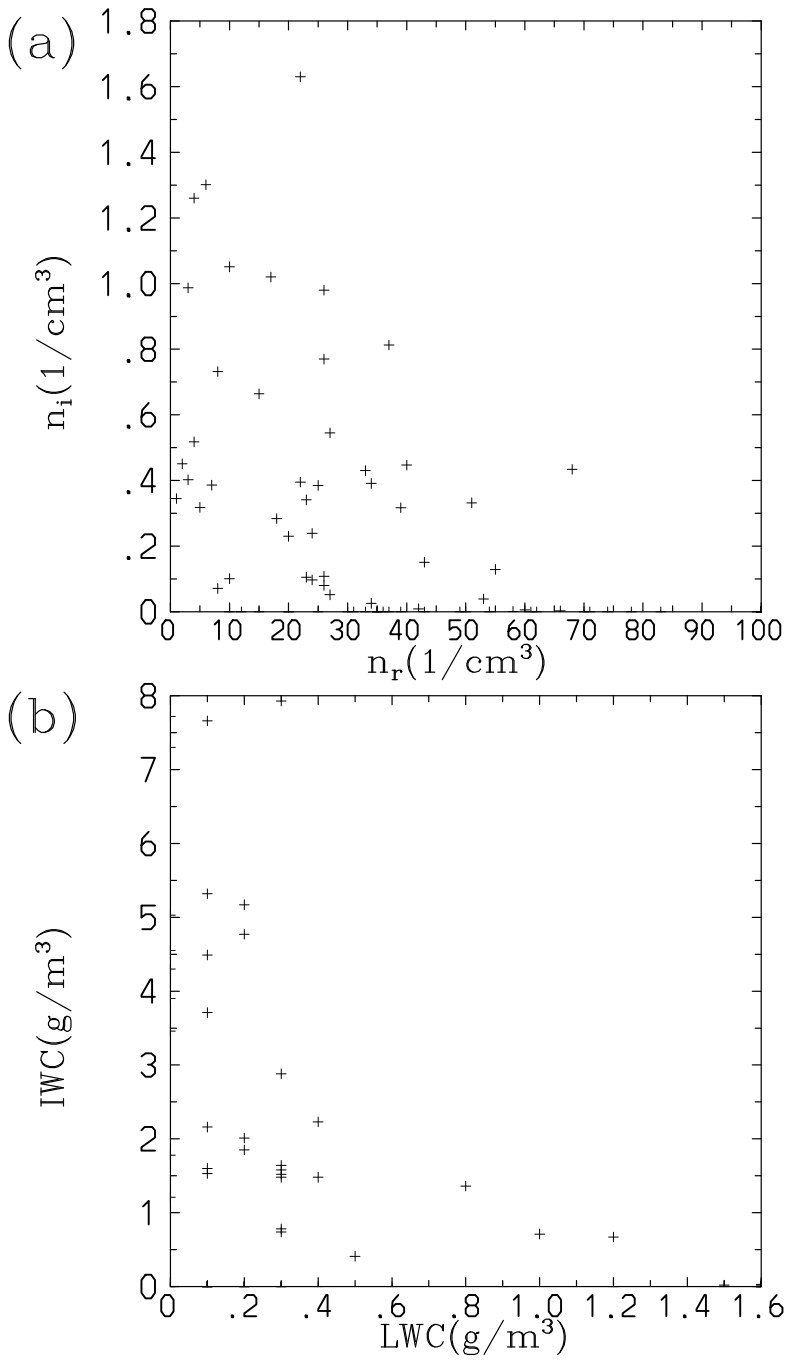

FIG. 4. Scatter plots between the liquid and the ice values observed during the ICE–T campaign. The values marked by + symbol are measurements for updraft cores: (a) particle number density ($1/cm^3$), (b) water content (g/m^3). Data is from Table 1 of Lawson *et al.* (2015).